

# EXTENDING DIGITAL WAVEGUIDES TO INCLUDE MATERIAL MODELLING

Marc Aird

Joel Laird

Dept. Of Mathematical Sciences  
University Of Bath  
mapma@maths.bath.ac.uk

Digital Music Research Group  
University Of Bristol  
Joel@qxlva.com

## ABSTRACT

Digital Waveguides have been extensively used for musical instrument and room acoustics modelling. They can be used to form simplistic models for ideal wave propagation in one, two and three dimensions. Models in 1D for string and wind instrument synthesis and more recently a model for a drum, realised by interfacing 2D and 3D waveguide meshes, have been presented [1]. A framework is thus in place for the virtual construction of new or abstract musical instruments. However, straight-forward waveguides and waveguide meshes behave in an extremely ideal nature and phenomena such as stiffness and internal friction are often compromised or ignored altogether. In this paper we discuss and evaluate models which incorporate material parameters. We review a 1D bar model, and then present a 2D extension to model plates. We also discuss the problem of modelling frequency dependent damping, by describing a waveguide model of a visco-elastically damped string.

## 1. INTRODUCTION

Current digital waveguide string models have incorporated non-linear phase filters to simulate stiffness [2], while IIR lowpass loop filters placed at the waveguide terminations can be used to simulate the frequency dependent losses observed in real strings [3]. In this paper we begin discussions on how such phenomena can be explicitly modelled within the waveguide framework. We discuss waveguide models which are equivalent to Finite Difference Schemes (FDS) derived from the underlying Partial Differential Equations (PDE).

We begin by describing a modified waveguide formulation involving interleaved waveguides. Using this method we are then able to describe a model for a vibrating bar, and extend this to include 2D models of vibrating plates. We then proceed to discuss how we may introduce frequency dependent damping models. We show how we may include some rudimentary damping, and how we may introduce additional dispersion to 1D waveguide models.

### 1.1. Interleaved Waveguides

The theory of interleaved waveguides was first introduced in [4] as an alternative waveguide model for the standard 1D wave equation and we summarise its construction here. Using an interleaved waveguide gives us access to two sets of wave variables; in the original formulation the two variables were voltage  $U$  and current  $I$ . The interleaved waveguide structure is shown in Figure 1. Each unit of delay has been split into two half-unit delay lines with a sign inversion, and a series junction had thus been inserted. The wave variables are related as follows. If we denote a left-going wave by superscripting with a (+) and a right going wave with a (-)

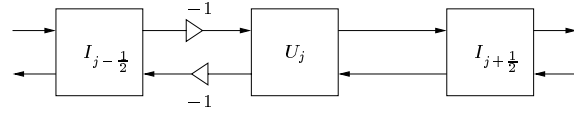


Figure 1: Interleaved Waveguide.

then

$$\begin{aligned} U^+ &= ZI^+ \\ U^- &= -ZI^- \end{aligned}$$

where  $Z$  is the waveguide impedance, with admittance  $Y = 1/Z$ . This is analogous to the relationship between force and velocity waves. Furthermore, in an interleaved delay line, the incoming waves to a scattering junction  $j$  can be expressed as the outgoing waves at neighbouring junctions for current-like waves,

$$\begin{aligned} I_{0,j}^+ &= -I_{1,j+\frac{1}{2}}^- \left(n - \frac{1}{2}\right), \\ I_{1,j}^- &= -I_{0,j-\frac{1}{2}}^+ \left(n - \frac{1}{2}\right), \end{aligned}$$

and for voltage-like waves,

$$\begin{aligned} U_{0,j}^+ &= U_{1,j+\frac{1}{2}}^- \left(n - \frac{1}{2}\right), \\ U_{1,j}^- &= U_{0,j-\frac{1}{2}}^+ \left(n - \frac{1}{2}\right). \end{aligned}$$

That is current-like waves travel with a sign inversion. Thus we inter-change between current and voltage waves each half time step (and each half spatial step). It has been shown in [4] that this alternate waveguide structure, which gives us access to two sorts of wave variable via the interconnection of series and parallel junctions, is equivalent to a FDS for the decoupled wave equation,

$$\left. \begin{aligned} \rho \frac{\partial i}{\partial t} + \frac{\partial u}{\partial x} &= 0 \\ \frac{1}{F} \frac{\partial u}{\partial t} + \frac{\partial i}{\partial x} &= 0 \end{aligned} \right\} \Rightarrow \frac{\partial^2 u}{\partial t^2} = \frac{F}{\rho} \frac{\partial^2 u}{\partial x^2}.$$

This technique of decoupling equations to give access to two sorts of variable is vital to the development of coupled waveguide networks for the more difficult 4<sup>th</sup> order PDE representing motion in an ideal bar.

## 2. A MODEL FOR AN IDEAL VIBRATING BAR

In this section we briefly review the work presented in [5] which described a model for an ideal bar using the interleaved waveguides described above. The method was first introduced in [4]. We are now also able to present a slightly more detailed analysis of the performance of the model.

## 2.1. The Euler-Bernoulli Equation for the Ideal Bar

The Euler-Bernoulli equation for transverse displacement  $u(x, t)$  of a stiff bar is

$$\frac{\partial^2 u}{\partial t^2} = -\frac{EI}{\rho A} \frac{\partial^4 u}{\partial x^4}, \quad (1)$$

where  $\rho$  is the materials density,  $E$  its Young's Modulus,  $A$  is the bar's cross-sectional area, and  $I$ , the moment of gyration about the beams perpendicular axis [6]. We consider harmonic travelling wave solutions of the form  $u = Ce^{i(kx-wt)}$ , where  $w$  is the frequency of the harmonic wave travelling at speed  $c = w/k$ . By substituting this solution into equation (1) we are able to calculate the frequency dependent wave speed

$$c(w) = \left(\frac{EI}{\rho A}\right)^{\frac{1}{4}} \sqrt{w}.$$

Thus the presence of only bending stiffness as a restoring force causes the wave speed to increase with frequency (from zero) as shown in the left hand plot of Figure 2, much unlike the case of an ideal string where all waves travel with the same speed. There are

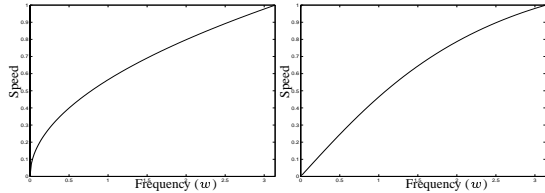


Figure 2: (a)-Frequency Dependent Wave Speed for an Ideal Bar. (b)-Dispersion in Bar Model

three types of boundary condition for a finite bar resulting from three different types of termination, free, supported (hinged) or clamped. Application of the the simplest of these, simply supported, results in the following sequence of resonant modes (in  $Hz$ )

$$f_n = \frac{\pi}{2L^2} \sqrt{\frac{EI}{\rho A}} n^2, \quad (2)$$

where  $L$  is the length of the bar.

## 2.2. Digital Waveguide Model For A Stiff Bar

The digital waveguide model for the stiff bar is realised by considering the de-coupled version of equation (1),

$$\begin{aligned} \frac{\partial v}{\partial t} &= -\frac{1}{\rho A} \frac{\partial^2 m}{\partial x^2} \\ \frac{\partial m}{\partial t} &= EI \frac{\partial^2 v}{\partial x^2}. \end{aligned}$$

Here,  $v = \frac{\partial w}{\partial t}$  is the beam's transverse velocity, while  $m$  may be interpreted as a bending moment. By applying centred differences to these equations we arrive at the following difference scheme,

$$\begin{aligned} V_j(n+1) - V_j(n) &= \\ & -\frac{\mu}{\rho A} \left[ M_{i+1}(n + \frac{1}{2}) - 2M_i(n + \frac{1}{2}) + M_{i-1}(n + \frac{1}{2}) \right] \\ M_i(n + \frac{1}{2}) - M_i(n - \frac{1}{2}) &= \\ & \mu EI [V_{i+1}(n) - 2V_i(n) + V_{i-1}(n)], \end{aligned} \quad (3)$$

where we define  $\mu = \frac{T}{\Delta x}$  for time step  $T = \frac{1}{f_s}$  and spatial step  $\Delta$ , and where  $f_s$  is the sample rate of the simulation. The dispersion of such a scheme may be easily computed [7] and is shown

Mode	Theoretical	Modelled	Error
$f_1$	11.56	11.5	0.06
$f_2$	46.26	45.5	0.70
$f_3$	104.09	103.0	1.09
$f_4$	185.05	182.5	2.55
$f_5$	289.14	284.5	4.64
$f_6$	416.37	408.5	7.87
$f_7$	566.72	554.0	12.72

Table 1: Comparing measured and real resonant modes (in  $Hz$ ) for bar model.

in the right hand plot of Figure 2 to compare favourably to the desired dispersion. The digital waveguide model is constructed by coupling two interleaved waveguides and is summarised in Figure 3. By placing each waveguide one spatial position out of sync with each other we enable access to each of the wave variables  $V$  (a voltage-like variable) and  $M$  (a current-like variable) at each spatial position. The coupling is performed using two waveguide connections, each carrying a sign inversion.

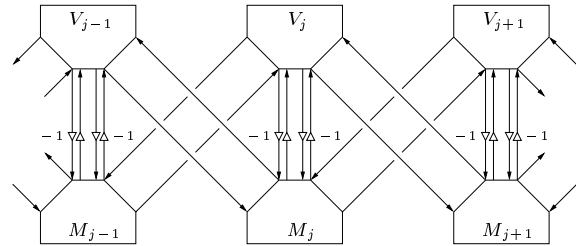


Figure 3: Digital Waveguide Bar.

derivation of the equivalence of this waveguide structure with the FDS of equation (3) can be found in [4] [5] and we omit them here due to space constraints. To summarise the equivalence we state that we must set the total junction impedance at a series  $M$  junction to

$$Z_J = 4Z = \frac{2}{EI\mu},$$

and the total junction admittance at a parallel  $V$  junction to

$$Y_J = 4Y = \frac{2\rho A}{\mu}.$$

This equations may be solved by setting  $Y = \sqrt{\rho A EI}$ , with  $Z = 1/Y$  and setting

$$\mu = \frac{1}{2} \sqrt{\frac{\rho A}{EI}}.$$

## 2.3. Simulation Example

We now present the results of a simulation of a bar of length  $1m$ , with a square cross section of height  $0.005m$ . We chose to model steel bar whose material parameters are  $E = 1.4 \times 10^{12} N/m^2$  and  $\rho = 53800 kg/m^3$ . With the sample rate set at  $f_s = 44100 Hz$  the resultant model employs a spatial step size of approximately  $\Delta = 1/55m$ . Shown in Table 1 are the results of the simulation showing a reasonable level of accuracy when compared to the desired mode positions as calculated using equation (2).

### 3. A 2D STIFF PLATE MODEL

In this section we formulate a straightforward extension of the waveguide bar model into 2D. We begin by describing in part the theory behind the vibratory motion of a stiff plate. The complete theory is quite complex; each edge of a rectangular plate, for example, can have any of three boundary conditions (free, clamped, and simply supported), resulting in 27 different combinations, with each leading to a different set of vibrational modes [6]. In this paper we only describe a simply supported rectangular plate, and note that the difficulties expressed above in finding an analytical solution in 2D plate dynamics suggests an accurate modelling technique would be extremely useful.

#### 3.1. The Stiff Plate Equations

Denoting transverse displacement by  $u(x, y, t)$ , the equation of motion for a vibrating plate is

$$\frac{\partial^2 u}{\partial t^2} + \frac{Eh^2}{12\rho(1-\nu^2)} \nabla^4 u = 0, \quad (4)$$

where  $h$  is the plate thickness,  $\rho$  is the density,  $E$  is Young's Modulus,  $\nu$  is Poisson's ratio and  $\nabla^4$  represents

$$\nabla^4 = \frac{\partial^4}{\partial x^4} + 2 \frac{\partial^4}{\partial x^2 \partial y^2} + \frac{\partial^4}{\partial y^4}$$

in cartesian coordinates. Writing  $u(x, y, t) = U(x, y)e^{i\omega t}$  yields the time reduced equation

$$(\nabla^2 - k^2)(\nabla^2 + k^2)U = 0,$$

where  $k^2 = \sqrt{\frac{12\rho(1-\nu^2)}{Eh^2}} \omega$ . Note, that we are now dealing with the 2D frequency vector  $\underline{\omega} = (\omega_x, \omega_y)^t$ . The frequency dependent speed of wave propagation can thus be calculated as

$$c(\underline{\omega})^2 = \sqrt{\frac{Eh^2}{12\rho(1-\nu^2)}} |\underline{\omega}|. \quad (5)$$

A contour plot of the true dispersion characteristics of the ideal plate are shown in Figure 4.

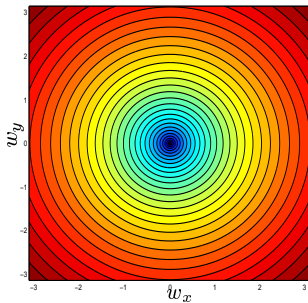


Figure 4: Dispersion for 2D plate.

As was mentioned above, the variety of possible boundary conditions, together with the complexity of the system, means that complete analytical solutions are either time-consuming, or difficult to achieve. Thus for this study we consider only a simply supported rectangular plate of length  $a$  and width  $b$ , whose resonant modes may be calculated from

$$f_{mn} = \frac{\pi}{2} \sqrt{\frac{Eh^2}{12\rho(1-\nu^2)}} \left[ \left(\frac{n}{a}\right)^2 + \left(\frac{m}{b}\right)^2 \right]. \quad (6)$$

It is important to note that we may also deduce the modes of an simply supported ideal bar from this by setting  $\nu = 0$  and  $n = 0$ , thus neglecting twisting moments and the contribution from the second dimension.

#### 3.2. Finite Difference Schemes for the Stiff Plate Equation

A digital waveguide mesh model which is entirely equivalent to a stable FDS for the 2D plate equation can be derived in an analogous fashion to the 1D case for an ideal bar. A centred FDS for equation (4) is achieved by applying finite differences over a regular square grid to the decoupled equation

$$\begin{aligned} \frac{\partial v}{\partial t} &= -\frac{1}{12\rho(1-\nu^2)} \nabla^2 m \\ \frac{\partial m}{\partial t} &= Eh^2 \nabla^2 v, \end{aligned} \quad (7)$$

for velocity waves  $v = \frac{\partial u}{\partial t}$ . It should be clear that this decoupled equation is also ideally suited when dealing with cases where the material parameters may vary spatially (as in the case with wood). The resultant FDS for the discrete variables  $V$  and  $M$  is as follows,

$$\begin{aligned} V_{i,j}(n+1) - V_{i,j}(n) &= \\ &= -\frac{1}{l} \mu \left[ M_{i,j+1}(n + \frac{1}{2}) - 2M_{i,j}(n + \frac{1}{2}) + M_{i,j-1}(n + \frac{1}{2}) \right] \\ &= -\frac{1}{l} \left[ M_{i-1,j}(n + \frac{1}{2}) - 2M_{i,j}(n + \frac{1}{2}) + M_{i+1,j}(n + \frac{1}{2}) \right], \\ M_{i,j}(n + \frac{1}{2}) - M_{i,j}(n + \frac{1}{2}) &= \\ &= -c\mu \left[ V_{i,j+1}(n) - 2V_{i,j}(n) + V_{i,j-1}(n) \right] \\ &= -c\mu \left[ V_{i-1,j}(n) - 2V_{i,j}(n) + V_{i+1,j}(n) \right], \end{aligned} \quad (8)$$

where  $\mu = \frac{T}{\Delta^2}$  and  $\frac{1}{l} = \frac{1}{12\rho(1-\nu^2)}$ ,  $c = Eh^2$ . By expressing the FDS in this form it is clear that, as was the case with the waveguide bar model, any plate model must be comprised of two coupled waveguide meshes. We shall describe such a construction later, but first, let us consider the dispersion properties of the above FDS. The spectral amplification factor [7],  $G(\underline{\omega})$ , may be calculated by solving the following quadratic

$$G(\underline{\omega})^2 + (B - 2)G(\underline{\omega}) + 1 = 0,$$

where for a square mesh geometry

$$\begin{aligned} B &= \frac{Eh^2}{12\rho(1-\nu^2)} \mu^2 \left[ 2 \cos(2w_x) + 2 \cos(2w_y) \right. \\ &\quad \left. - 16 \cos(w_x) - 16 \cos(w_y) \right. \\ &\quad \left. + 4 \cos(w_x + w_y) + 4 \cos(w_x - w_y) + 20 \right]. \end{aligned} \quad (9)$$

The resultant amplification factor is always complex and the dispersion is calculated by normalising it's argument and shown as a contour plot in Figure 5. Note the directional (as well as frequency) dependence of the dispersion. Wave speeds in the diagonal direction seem consistent with the desired wave speed indicated in Figure 4, but performance in the axial directions is poor. This is analogous to the case of a regular 2D mesh modelling the non-stiff 2D wave equation. Thus it seems reasonable to assume that using a triangular mesh geometry will yield a FDS with direction independent dispersion. Such a FDS can quite easily be derived, and it's dispersion can be calculated using

$$\begin{aligned} B &= \frac{Eh^2}{12\rho(1-\nu^2)} \mu^2 \frac{4}{9} \left[ 42 - 20 \cos(w_x) + 4 \cos(\sqrt{3}w_y) \right. \\ &\quad \left. - 20 \cos \frac{1}{2}(w_x + \sqrt{3}w_y) - 20 \cos \frac{1}{2}(w_x - \sqrt{3}w_y) \right. \\ &\quad \left. + 4 \cos \frac{1}{2}(3w_x + \sqrt{3}w_y) + 4 \cos \frac{1}{2}(3w_x - \sqrt{3}w_y) \right. \\ &\quad \left. + 2 \cos(2w_x) + 2 \cos(w_x + \sqrt{3}w_y) + 2 \cos(w_x - \sqrt{3}w_y) \right]. \end{aligned} \quad (10)$$

in place of equation (9). The desired improvements to the dispersion characteristics are quite clearly evident in Figure 6.

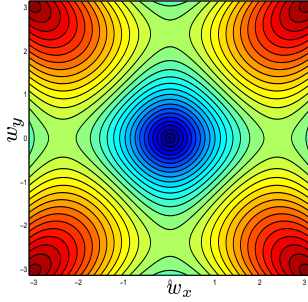


Figure 5: Dispersion in 2D plate model using square mesh.

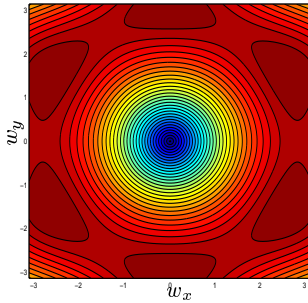


Figure 6: Dispersion in 2D plate model using triangular mesh.

### 3.3. 2D Waveguide Plate Model

As was discussed in the previous section, we now describe the construction of a waveguide model which is equivalent to the FDS of equation (8) by coupling two waveguide meshes. One mesh will carry the wave variable  $V$ , while the other carries the variable  $M$ . The model is constructed using two interleaved waveguide grids, coupled together at alternate wave variable junctions using four waveguides, each carrying a sign inversion. It should be noted that a waveguide mesh model for the more detailed Mindlin plate theory has also been derived in [4]. This is a direct extension of the 1D technique. Again, we choose not to include the details of the equivalence and summarise the results as follows.

It can be shown, by application of the relationships of Section 1.1, that the coupled waveguide mesh plate model is equivalent to the required FDS by setting the total junction impedance at a series  $M$  junction to

$$Z_J = 8Z = \frac{2}{Eh^2\mu},$$

and the total junction admittance at a parallel  $V$  junction to

$$Y_J = 8Y = \frac{12\rho(1-\nu^2)}{2\mu}.$$

This equations may be solved by setting  $Y = \sqrt{12Eh^2\rho(1-\nu^2)}$ , with  $Z = 1/Y$  and setting

$$\mu = \frac{1}{4} \sqrt{\frac{12\rho(1-\nu^2)}{Eh^2}}.$$

### 3.4. Simulation Example

We carried out a simulation for a square steel plate of length  $a = 0.5m$ , with thickness  $h = 0.005m$ ,  $E = 1.4 \times 10^{12}N/m^2$ ,  $\rho = 53800kg/m^3$  and  $\nu = 0.3$ . The resulting spatial step size was  $\Delta = 0.01323m$ , giving a mesh of size  $38 \times 38$  nodes. The results of the simulation are summarised in Table 2 where the expected mode frequencies were calculated using equation (6). The results appear to be reasonably good, particularly the tuning of the fundamental, and the subsequent errors seem consistent with the dispersion error observed in Figure 5.

Mode	Theoretical	Modelled	Error
$f_{11}$	96.9932	97	0.0068
$f_{12} = f_{21}$	242.4831	241	1.4831
$f_{22}$	387.9729	383	4.9729
$f_{13} = f_{31}$	484.9662	479	5.9662
$f_{23} = f_{32}$	630.4560	623	7.456
$f_{14} = f_{41}$	824.4425	809	15.4425
$f_{33}$	872.9391	861	11.9391

Table 2: Comparing measured and real resonant modes (in Hz) for plate model.

## 4. INCLUDING FREQUENCY DEPENDENT DAMPING

We have shown how it is possible to design waveguide models which include bending stiffness. We have thus been able to introduce some material specific parameters. Another aspect which dictates the quality of the sound of a particular material is damping, which is typically frequency dependent. In this section we discuss how it could be possible to introduce damping to waveguide models by placing the resonator on some visco-elastic foundation designed to match the visco-elastic response of a given material [8]. This idea was initially suggested and demonstrated in [9], and we wish to derive a waveguide formulation of those ideas.

### 4.1. Modelling a String on a Visco-elastic Foundation

Consider the simplest case of a string placed on a viscoelastic foundation comprised of a spring and dash-pot in parallel. The equation of motion of such a system is

$$F \frac{\partial^2 u}{\partial x^2} - Gu - g \frac{\partial u}{\partial t} = \rho \frac{\partial^2 u}{\partial t^2}, \quad (11)$$

where  $F$  is string tension,  $\rho$  it's density,  $G$  is spring stiffness and  $g$  is the viscosity coefficient. This has been used as an approximate damping term in [10]

We use centred differences to directly derive a FDS for equation (11) with the discrete variable  $U_j(n)$ .

$$\begin{aligned} &U_j(n+1) - 2U_j(n) + U_j(n-1) = \\ &\frac{F}{\rho} \frac{T^2}{\Delta^2} [U_{j+1}(n) - 2U_j(n) + U_{j-1}(n)] \\ &- T^2 \frac{G}{\rho} U_j(n) - T \frac{g}{\rho} [U_j(n) - U_j(n-1)]. \end{aligned} \quad (12)$$

Shown in Figure 7 is a waveguide model for the viscoelastic string. It is constructed from an ordinary waveguide string model by including a self-loop with sign inversion (attached with impedance  $R_s$ ), and a hole (of impedance  $R_d$ ), to each junction. The structure

can be shown to be equivalent to the FDS above by choosing the following junction impedances,

$$R_s = \frac{2GT^2}{4\rho - 2gT - GT^2}, R_d = \frac{4gT}{4\rho - 2gT - GT^2},$$

with spatial step calculated from

$$\Delta = T \sqrt{\frac{4F}{4\rho - 2gT - GT^2}}.$$

Note how in the absence of the visco-elastic foundation we would have  $R_s = R_d = 0$ , with  $\Delta = T \sqrt{F/\rho}$ , and the model would reduce to that of a standard waveguide string.

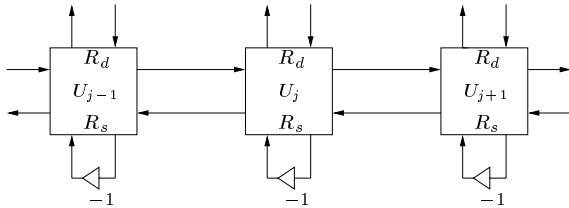


Figure 7: Viscoelastic Waveguide.

## 4.2. Simulation Examples

For a simulation example we consider a model for a string on an elastic foundation. The presence of an elastic foundation of stiffness  $G$  introduces dispersion such that the frequency and wave number are related by

$$\omega^2 = c^2 \left( k^2 + \frac{G}{F} \right), \quad (13)$$

where  $c = \sqrt{F/\rho}$ . From this we may predict the fundamental frequency for a string of length  $L$  as

$$f_1 = \frac{c}{2\pi} \left[ \left( \frac{\pi}{L} \right)^2 + \frac{G}{F} \right]^{\frac{1}{2}}. \quad (14)$$

Note that putting  $G = 0$  in both equations (13) and (14) returns to the case of an ideal string. Thus we conclude that foundation stiffness causes an increase in the fundamental. Furthermore equation (13) shows us that initial resonances will be spaced quite close together, but that as frequency increases the spacing between partials will approach a limiting value, giving a harmonic series. This is demonstrated using our model in Figure 8. One curve shows the spectral output of a regular waveguide string, the other a string on an elastic foundation. We observe an increased fundamental in the latter case and a spread of frequencies which approaches that of the ideal string for higher frequencies. Furthermore Table 3

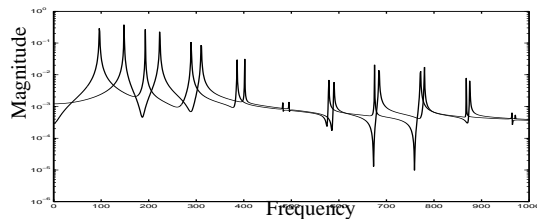


Figure 8: Comparison of a string with a string on an elastic foundation.

shows how the model accurately represents the increased fundamental frequency.

Stiffness $G$	Model Frequency	Theoretical Frequency
0	96	96.1769
$10^2$	96	96.2427
$10^3$	97	96.8331
$10^4$	103	102.5501
$10^5$	148	148.0377

Table 3: Comparing measured and real fundamental frequencies for a String on an Elastic Foundation

## 5. CONCLUSIONS AND FUTURE WORK

This paper has discussed approaches to introducing increased realism into digital waveguide models. We have introduced models which include bending stiffness for simulations of bars and plates. Furthermore we have introduced a model for a string on a visco-elastic foundation as a pre-cursor to research into waveguide models including material specific frequency-dependent damping.

The opportunities for future work in this area are quite vast. The models of Sections 2 and 3 should be extended to cover stiff strings and membranes. Also the models could cope with materials exhibiting direction-dependent parameters such as wood. In Section 4 it should be possible to extend the ideas to include more complicated viscoelastic foundations, as suggested in [9]. Finally these techniques could be incorporated with the mesh interfacing technique described in [1] and [3] so that very realistic models of complete musical instruments could be achieved.

## 6. REFERENCES

- [1] Aird, M, Laird, J, Fitch, J, "Modelling a drum by interfacing 2-d and 3-d waveguide meshes", Proc. International Computer Music Conference, 2000.
- [2] Van Duyne, S. A., Smith, J. O., "A simplified approach to modeling dispersion caused by stiffness in strings and plates", Proc. International Computer Music Conference, 1994.
- [3] Laird, Joel, "The Physical Modelling Of Drums Using Digital Waveguides", PhD Thesis, Bristol University, October 2001.
- [4] Bilbao, Stefan, "Wave and Scattering Methods for the Numerical Integration of Partial Differential Equations", PhD thesis, Stanford University, March 2001. Available at <http://www-ccrma.stanford.edu/bilbao/>.
- [5] Aird, M, Laird, J, "Towards Material Modelling in Physical Models Using Digital Waveguides", Proc. Music Without Walls? Music Without Instruments? June 2001.
- [6] Graff, K. F., "Wave motion in elastic solids", Oxford University Press 1975.
- [7] Strikwerda, J., C., "Finite Difference Schemes and Partial Differential Equations" Wadsworth and Brooks, 1989.
- [8] Tschoegl, N. W., "The Phenomenological Theory of Linear Viscoelastic Behaviour", Springer-Verlag, 1989.
- [9] Djoharian, P, "Shape and material design in physical modelling sound synthesis", Proc. International Computer Music Conference, 2000.
- [10] Chaigne, A., Doutaut, V., "Numerical simulations of xylophones. I. Time-domain modelling of the vibrating bars", J. Acoust. Soc. Am. 101(1), January 1997.